Inorganic Chemistry

Article

pubs.acs.org/IC

C−H Activation by Multiply Bonded Complexes with Potentially Noninnocent Ligands: A Computational Study

Olayinka A. Olatunji-Ojo and Thomas R. Cundari*

Department of Chemistry and Center for Advanced Scientific Computing and Modeling (CASCaM), University of North Texas, 1155 Union Circle, #305070 Denton, Texas 76203-5070, United States

Supporting Information

ABSTRACT: Second- and third-row (typically precious metals) transition metal complexes are known to possess certain electronic features that define their structure and reactivity and are usually not observed in their first-row (base metal) congeners. Can these electronic features be conferred onto first-row transition metals with the aid of noninnocent and/or very high-field ligands? In this research, the impact upon methane C−H bond activation was modeled using the dipyridylazaallyl (smif) supporting ligand for late, first-row transition metal (M) imide, oxo, and carbene complexes (M = Fe, Co, Ni, or Cu; E = O, NMe, or CMe_2). Density functional theory calculations suggest that the combination of smif with iron and the oxo activating ligand is the most energetically favorable complex for methane C−H activation. A change in the preferred transition state for methane C−H activation from [2+2] addition to hydrogen atom abstraction was observed upon going from Fe to Cu and for Fe as compared to precious metals. Contrary to expectations, it was the imide ligand rather than the dipyridylazaallyl ligand that was found to possess redox "noninnocent" characteristics.

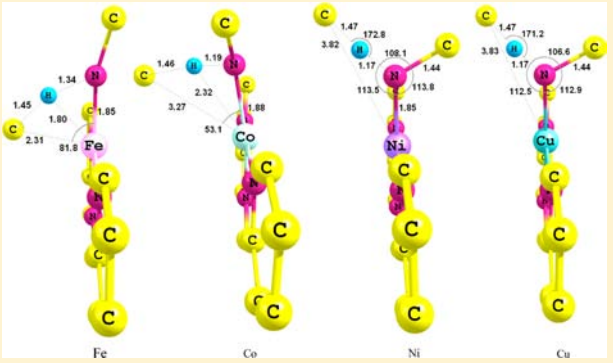

1. INTRODUCTION

Carbon−hydrogen bond activation and functionalization has been an important topic in catalysis for the past few decades.[1−7] Converting hydrocarbons, especially alkanes, to products with higher functionality and hence applicability via direct routes (as opposed to multistep syntheses via synthesis gas or routes that involve, for example, initial halogenation followed by bond coupling) is very important albeit difficult to achieve. Processes such as the conversion of methane, the primary component of natural gas, to methanol require carbon−hydrogen bond activation.[8−13] The challenge of C−H bond activation can be attributed to the chemical inertness of alkanes and their thermodynamic stability arising from their strong C−H bonds.[1−12] Also, selectivity is important with C−H bond activation. Partial oxidation products (such as methanol) are preferable over more extensively oxidized byproducts.

The desire to selectively functionalize strong C−H bonds under mild conditions has led to the intense study of transition metal catalysis.[1,5,14−17] A family of complexes that has been found to activate alkanes is metal imides: $L_nM{=}NR$.[2,5,6,14,18−28] Early first-row transition metal-imide complexes (typically in the highest formal oxidation state of the metal) are well-known in the literature; however, isolated late first-row transition metal-imide complexes are rare[21,23] but are becoming more well-studied, both computationally and experimentally.[21−23,29−38]

Late first-row transition (Fe, Co, Ni, Cu, Zn) or base metals have traditionally been used less than precious metals in industrial and fine chemical catalysis. The different reactivity profile of 3d metals compared to those of their precious metal analogues is obviously due to the different electronic properties of the latter (i.e., 4d and 5d) metals. Wolczanski and coworkers have proposed that a key electronic feature displayed by 3d metals in relation to their heavier counterparts is a higher density of states (giving rise to a greater range of reactivity and thus potentially reduced selectivity) and a reduced tendency to perform two-electron redox chemistry (e.g., oxidative addition and reductive elimination) as opposed to $1e^-$ (radical, bond scission, etc.) chemistry.[39,40] It is, therefore, desirable to develop base metal replacements with electronic properties comparable to those of precious metal catalysts.[41] One may thus inquire whether the favorable electronic properties of precious metal catalysts can be conferred onto 3d replacements. Alternatively, by using a ligand with high crystal field strength, may the density of states seen in 4d and 5d complexes be mimicked by 3d congeners, thus making 3d metal complexes more "precious"?

Noninnocent ligands have been used to tune the reactivity and properties of transition metals.[39,42,43] Noninnocent ligands (NILs) or redox-active ligands are ligands with potentially variable oxidation states. The ligation of redox-active ligands to transition metals has been shown to modify the reactivity and electronic properties of both components.[44−51] The goal of this

Received: April 1, 2013
Published: June 26, 2013

   dx.doi.org/10.1021/ic400804x | Inorg. Chem. 2013, 52, 8106−8113

research is to model methane C−H bond activation by 3d transition metal-imide complexes with high-field supporting ligands that are potentially noninnocent.

The potentially noninnocent ligand used in this study is the dipyridylazaallyl (termed smif) ligand. Previous experimental and computational studies by Wolczanski, Cundari, and collaborators show smif to be a very high-field ligand with redox-active properties (Figure 1).[39,52−55] Frazier et al. found

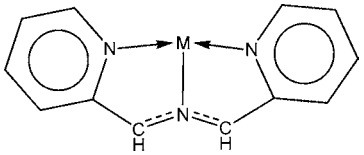

Figure 1. Potentially noninnocent monoanionic dipyridylazaallyl (smif) ligand.

some interesting electronic features in the smif ligand.[52,53] Specifically, the redox activity of the smif ligand was revealed through a molecular orbital analysis of the bis(smif) complexes of Fe, Co, and Ni. The Δ_o for diamagnetic $(smif)_2Fe$ was estimated to be ∼18000 cm^{-1}. For the singlet $(smif)_2Fe$ and triplet $(smif)_2Ni$ complexes, experiments indicate smif to be redox innocent, that is, monoanionic. However, for the doublet $(smif)_2Co$ complex, the extra (relative to $(smif)_2Fe$) electron occupies a ligand π^* rather than a metal-based e_g^* orbital, effectively changing the average charge on the smif from −1 to −1.5 and thus making the metal ion more akin to a Co^{III} formal oxidation state.[52] Noninnocence of the smif ligand was also observed by Frazier and co-workers for the $(smif)_2Cr$ complex, which was categorized as $(smif^{-})(smif^{2-})Cr^{III}$.[53] Normalized K-edge spectra of the $(smif)_2Cr$ and $(smif)_2Cr^{+}$ complexes indicate ligand-based oxidation for the neutral Cr complex. Both the neutral and cationic bis(smif) chromium complexes exhibited Δ_o of approximately 17500−19500 cm^{-1}.

Hachmann et al. conducted a theoretical study on the electronic properties of bis(smif) ligation about 3d transition metals.[54] A thorough investigation of the structure, magnetism, and oxidation states of these complexes led to some interesting results. First, $M(smif)_2$ complexes can possess multiple low-lying, nearly degenerate electronic states. These researchers also found that there are slight geometrical and oxidation state changes depending on the metal, corroborating the non-innocent behavior that is sometimes exhibited by the smif ligand and that was inferred from crystallographic and spectroscopic studies. Hachmann et al. also concluded that with the appropriate selection of metal and ligand, as well as modification of the latter, the smif ligand could be used to control electronic properties of the resulting complex,[54] which is, of course, very desirable in a catalyst design scenario. An important consideration with respect to noninnocent ligand selection is whether the ligand will always exhibit redox noninnocence in different environments. Cowley and co-workers conducted a joint experimental and computational study on a (β-diketiminato)iron complex with end-on and side-on interaction with nitriles.[56] Although there was evidence of electron density transfer from the metal to the nitrile ligand, they concluded that backbonding was more likely than noninnocence of the nitrile ligand.[56]

Base metals considered in this research are iron, cobalt, nickel, and copper. Some precious metals (ruthenium, osmium, and palladium) were considered for comparison. Also, the studied complexes were modified such that the activating ligand of primary interest (E = NMe) was changed to other isoelectronic ligands (E = CMe_2, O).

2. COMPUTATIONAL METHODS

Density functional theory (DFT) calculations were performed using the Gaussian 09 package.[57] The M06[58] functional was used with two different basis sets: a double-ζ, all-electron, Pople-style 6-31+G(d)[59,60] basis set was used to model first-row transition metal complexes. Previous calculations on complexes with the smif supporting ligand and other organometallic complexes have shown accurate kinetic and thermodynamic results using the M06 functional and thus motivated the selection of this functional for the present study.[61,62] A pseudopotential/valence basis set approach was used for the palladium, ruthenium, and osmium calculations with the Stevens triple-ζ valence CEP-31G[63−65] basis set used for the metal center and the 6-31+G(d) basis set used for the main group elements. Simulations were conducted in the gas phase at standard temperature and pressure (298.15 K and 1 atm). Solvent effects were found to be minimal using the SMD solvation model with THF as the solvent. The energies reported are free energies in kilocalories per mole. The typical reaction pathway studied is shown in Figure 2. The radical rebound step following the hydrogen atom abstraction (HAA) route was assumed to be barrierless.

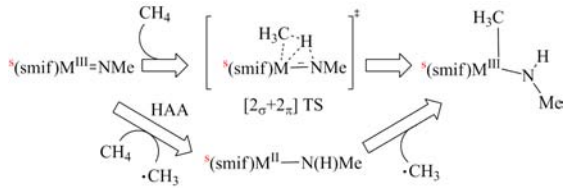

Figure 2. Reaction pathways modeled in this research; a superscript s denotes the lowest-energy spin state calculated for a stationary point. HAA denotes hydrogen atom abstraction route.

3. RESULTS AND DISCUSSION

A. Base Metals. The reaction pathways in Figure 2 were studied for base metals: (smif)M═NMe + CH_4 → (smif)M-(CH_3)(NHMe), where M = Fe, Co, Ni, or Cu. There are two plausible routes (based on literature precedent[1,4,13,14,16,66−68]) from the imide reactant to the four-coordinate amide product. One involves a four-centered $[2_\sigma+2_\pi]$ transition state (Figure 3). The other pathway is via an HAA transition state whereby

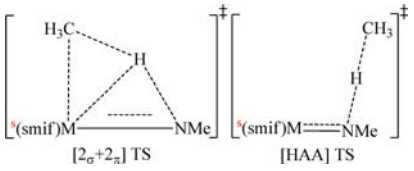

Figure 3. Transition state types modeled for (smif)M═NMe + CH_4 reaction.

H is abstracted directly from the methane by the nitrogen of the NMe ligand (Figure 3).[1,4,16] Unlike the $[2_\sigma+2_\pi]$ transition state, there is no direct involvement by the metal center in the C−H scission; however, the metal will play a role because HAA entails a formal reduction of the metal. The transition state (TS) types can be differentiated by computed properties such as geometries, bond lengths, and angles. For example, $[2_\sigma+2_\pi]$ TSs typically display a kite-shaped geometry, which is unlike the HAA TS. The $[2_\sigma+2_\pi]$ TSs typically possess N−H−CH_3

dx.doi.org/10.1021/ic400804x | Inorg. Chem. 2013, 52, 8106−8113

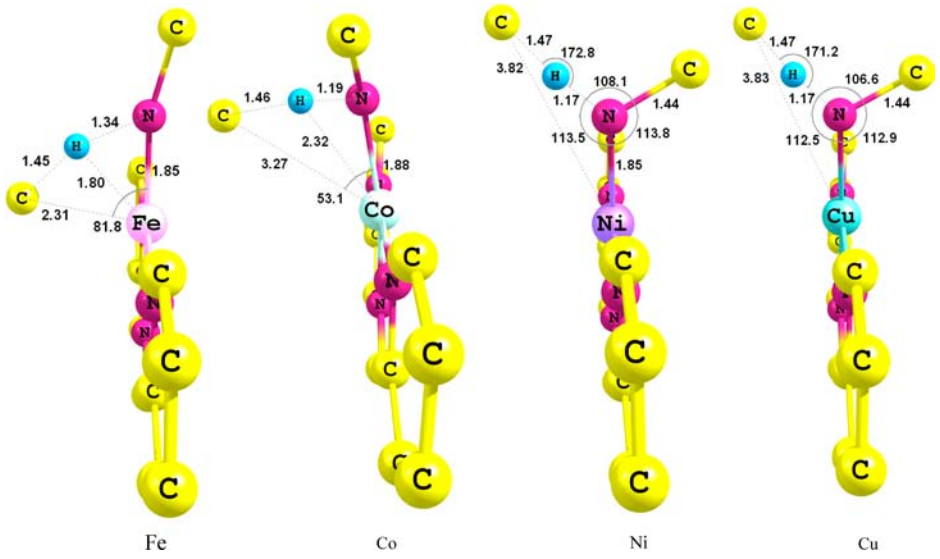

Figure 4. M06/6-31+G(d) calculated transition state geometries for methane C−H bond activation by (smif)M═NMe (M = Fe, Co, Ni, or Cu). All hydrogen atoms, except that being activated on methane, are omitted from the figure for clarity. Bond lengths are given in angstroms, bond angles in degrees.

Table 1. Calculated Lowest-Energy Spin States, Thermodynamics, and Kinetics of the (smif)M═NMe + CH_4 → (smif)M(CH_3)(NHMe) Reaction

	imide reactant spin state	TS spin state	four-coordinate amide product spin state	$\Delta G^{\ddagger}$ (kcal/mol)	ΔG_{rxn} (kcal/mol)	TS type
Fe	sextet	sextet	sextet	29.1	−9.6	$[2_\sigma+2_\pi]$
Co	triplet	triplet	singlet	37.0	1.1	$[2_\sigma+2_\pi]$ ↔ [HAA]
Ni	doublet	doublet	doublet	32.9	16.6	[HAA]
Cu	triplet	triplet	singlet	31.6	13.2	[HAA]

bond angles smaller than those of the HAA TSs, which are generally near linear about the transferring H. The carbon−metal−nitrogen bond angle in a $[2_\sigma+2_\pi]$ TS tends to be ∼80−90°, whereas the carbon−nitrogen−metal bond angle in the HAA TS is typically >100°.[1,2,16,19] Given these angular preferences, the metal−carbon bond distance in the $[2_\sigma+2_\pi]$ TS is typically less than 2.5 Å, while the metal−carbon bond length in the HAA TS is expected to be greater than 3.0 Å. Both the $[2_\sigma+2_\pi]$ and HAA TSs were modeled for *all complexes* to assess the preferred route of methane activation as a function of metal and activating ligand. Our discussion will primarily focus on the lowest-energy pathways indicated by the DFT simulations.

The ^{6}(smif)Fe═NMe + CH_4 → ^{6}(smif)M(CH_3)(NHMe) reaction was calculated to proceed via a $[2_\sigma+2_\pi]$ (Figure 4) pathway. The lowest-energy state was sextet for all the steps in the Fe-imide reaction pathway, thus implying spin conservation along the reaction coordinate. The activation energy was calculated to be 29.1 kcal/mol (versus separated reactants), and the free energy of the reaction was exergonic at −9.6 kcal/mol (Table 1). The hydrogen atom abstraction pathway was also calculated for the (smif)Fe-imide complex. Repeated transition state searches with differing starting guess geometries all collapsed to the $[2_\sigma+2_\pi]$ TS. When the geometry was constrained by fixing active site bond lengths and angles, an HAA pseudo-TS was obtained but was calculated to be 18.2 kcal/mol higher than the true (fully optimized) $[2_\sigma+2_\pi]$ TS shown in Figure 4. Consistent with the deduction that HAA is a high-energy pathway for ^{6}(smif)Fe═NMe, the endergonicity of the HAA reaction (ΔG_{HAA} = 15.6 kcal/mol, Table 2) contrasts the exergonicity of the $[2_\sigma+2_\pi]$ route (ΔG_{rxn} = −9.6 kcal/mol).

Table 2. Calculated Thermodynamics of the (smif)M═NMe + CH_4 → (smif)M-NHMe + $CH_3^\bullet$ Reaction

	imide spin state	three-coordinate amide spin state	ΔG_{HAA} (kcal/mol)[a]
Fe	sextet	quintet	15.6
Co	triplet	quartet	16.8
Ni	doublet	singlet	17.6
Cu	triplet	doublet	17.9

[a]HAA = hydrogen atom abstraction.

Pierpont and Cundari[16] studied methane C−H activation by metal-imide complexes with a β-diketiminate supporting ligand. For the ^{4}(β-diketiminate)Fe═NMe + CH_4 hydrogen atom abstraction route, the calculated reaction enthalpy was 19.8 kcal/mol. The HAA reaction enthalpy from this study, (smif)Fe═NMe + $H^\bullet$ → (smif)M-NHMe, is calculated as 16.7 kcal/mol.[16] Vaddadi[69,70] reported an HAA enthalpic barrier of 22 kcal/mol for methane activation by an intermediate-spin, three-coordinate ^{4}(β-diketiminate)Fe-imido. Assuming that $T\Delta S$ is ∼10 kcal/mol at STP, this suggests a hydrogen atom abstraction free-energy barrier of ca. 32 kcal/mol for ^{4}(β-diketiminate)Fe═NMe + CH_4, implying a kinetic advantage for the ^{6}(smif)Fe═NMe complex modeled here [$\Delta G^{\ddagger}$ ∼ 29 kcal/mol (Table 1)]. This may be reasonably ascribed to the high-spin nature of the smif imide complex (placing more spin density on the imide N), the effect of supporting ligand substitution, and/or an intrinsic mechanistic advantage for $[2_\sigma+2_\pi]$ over HAA pathways. We will return to these points below.

dx.doi.org/10.1021/ic400804x | Inorg. Chem. 2013, 52, 8106−8113

For the ^{3}(smif)Co=NMe and ^{3}(smif)Cu=NMe reactions with methane, reactant and transition states were triplets, but a spin "flip" was predicted for the products, which are both singlets. As the spin crossing occurred after the transition states, further refinement of the crossing points was not pursued.

Interestingly, for the cobalt-imide complex the methane activation TS lies (in a geometric sense) between the $[2_\sigma+2_\pi]$ and HAA prototypes as deduced from the computed bond lengths and angles (Figure 4). The $[2_\sigma+2_\pi]$ TS guesses for ^{3}(smif)Co=NMe + CH_4 converged to essentially the same TS obtained from HAA-like starting guesses. For the Cu-imide complex, however, the methane activation transition state was clearly of the HAA variety (Figure 4). The intermediacy of the modeled TS for the Co-imide/CH_4 reaction, which is between those calculated for the iron and copper derivatives that flank it, provides an important first clue to the sensitivity of the preferred C−H activation pathways to the specific metal−ligand combination. Moreover, computations imply that as one traverses toward later metals in the 3d series, there is a change in the preferred mechanism from a [2+2] pathway to an HAA route.

The calculated activation free energy was 37.0 kcal/mol for the triplet $([2_\sigma+2_\pi] \leftrightarrow [HAA])^{\ddagger}$ relative to methane + ^{3}(smif)Co=NMe and 31.6 kcal/mol for the triplet HAA TS for methane activation by ^{3}(smif)Cu=NMe. The free energies of these reactions (ΔG_{rxn}) to form ^{1}(smif)M(CH_3)(NHMe) were 1.1 and 13.2 kcal/mol for Co- and Cu-imide complexes, respectively (Table 1). The HAA free energy (ΔG_{HAA}) was calculated as 16.8 kcal/mol for Co-imide and 17.9 kcal/mol for Cu-imide (Table 2), which are thus ∼1−2 kcal/mol more endergonic than the value calculated for the Fe derivative.

For the activation of methane by ^{2}(smif)Ni=NMe, spin conservation was observed along the entire HAA reaction coordinate; the lowest-energy spin state calculated for all stationary points was a doublet. The activation free energy was calculated to be 32.9 kcal/mol, higher than the calculated activation energy of the iron-imide complex by 3.8 kcal/mol. The *enthalpic* activation barrier calculated by Pierpont and Cundari[16] for the ^{2}(β-diketiminate)Ni=imide + CH_4 reaction was 26.5 kcal/mol, whereas the enthalpic barrier for ^{2}(smif)-Ni=imide + CH_4 from this study was calculated to be 22.2 kcal/mol. Thus far, the smif supporting ligand displays a computed kinetic advantage over the β-diketiminate ligand with respect to methane activation. The calculated preferred TS type for methane activation by ^{2}(smif)Ni=NMe was the HAA variant (Figure 4). The $[2_\sigma+2_\pi]$ TS was isolated and calculated to be ∼19.0 kcal/mol higher than the HAA TS for these nickel complexes. The free energy of the HAA reaction was 16.6 kcal/mol (Table 2).

B. Ligand Modification. Two families of ligand modifications were modeled. First, we explored alteration of the NMe activating ligand by isovalent replacements, O and CMe_2. Second, substitution of smif backbone hydrogens with electron-withdrawing F and CF_3 groups was evaluated. The latter had almost no impact on the methane C−H activation barriers apart from an increase in $\Delta G^{\ddagger}$ due to steric reasons in the $[2_\sigma+2_\pi]$ barrier for a smif derivative in which *ortho* hydrogens are replaced by trifluoromethyls. Hence, our focus in the current paper is on the impact of the activating ligand.

The (smif)Fe-imide complex is computed to be the most favorable complex for methane C−H activation, kinetically and thermodynamically, among those studied thus far (Table 1). Although the calculated C−H activation free energy is experimentally attractive at 29.1 kcal/mol (as is the prediction of spin conservation along the pathway), modifications to ^{6}(smif)Fe=NMe were sought that would yield lower C−H activation barriers. First, the activating ligand (=NMe) was replaced with two other isovalent ligands: oxo (=O) and dimethylcarbene (=CMe_2). There is precedent in the literature for C−H activation by Fe−oxo complexes in biological systems, with available evidence pointing to an HAA mechanism.[71−75] Terminal Fe−oxo species are proposed as active species in hydroxylation catalysts for both heme (porphyrin) and non-heme systems. Iron−oxo (or ferryl, typically formulated as Fe^{IV}) species are the putative active species for the enzyme cytochrome P450, which catalyzes the aerobic oxidation of organic substances.

For the ^{6}(smif)Fe=O complex, as with the Fe=NMe congener, the lowest-energy multiplicity of all stationary points in the computed pathway was sextet, and the preferred reaction pathway was via a $[2_\sigma+2_\pi]$ TS. The preferred pathway calculated in the current situation is thus distinct from the putative HAA mechanism for ferryl-porphyrin intermediates in cytochrome P450. It is interesting to speculate whether the difference in mechanism is due to the lower iron coordination number in the smif models or the difference in formal oxidation states of the metal (formally Fe^{3+} in (smif)Fe=O). The activation energy was calculated to be 26.3 kcal/mol, 2.8 kcal/mol lower than that of the corresponding (smif)Fe=NMe complex. The free energy of the $[2_\sigma+2_\pi]$ reaction was −10.1 kcal/mol, which is 0.5 kcal/mol more exergonic than the value for the Fe=NMe complex (Table 3).

Table 3. Energetics of Methane Reactions with Fe(smif) Complexes with Different Activating Ligands[a]

	$\Delta G^{\ddagger}$ (kcal/mol)	ΔG_{rxn} (kcal/mol)	ΔG_{HAA} (kcal/mol)
^{6}(smif)Fe=O	26.3	−10.1	10.2
^{6}(smif)Fe=NMe	29.1	−9.6	15.6
^{4}(smif)Fe=CMe_2	34.3	−6.2	21.9

[a]All transition states are of the $[2\sigma+2\pi]$ type.

The (smif)Fe=CMe_2 presented very interesting results, quite distinct from those of its oxo and imide congeners. The lowest-energy reactant state was quartet, unlike the other Fe complexes which are sextets, presumably a reflection of greater covalency in iron−carbon versus iron−nitrogen/oxygen bonds. Also, a spin cross was observed *before* the $[2_\sigma+2_\pi]$ TS, which was calculated to have a sextet spin state. This is the first spin crossing before a C−H activation TS calculated thus far in this research (Figure 5). The activation energy was calculated to be 34.3 kcal/mol for the quartet surface, which is 8 kcal/mol higher than the oxo complex and ∼5 kcal/mol higher than the Fe-imide complex. The overall free energy of the reaction on the quartet surface was −6.2 kcal/mol (Table 3), which is less exergonic than the spin-conserving oxo and imide versions. Given these energetic parameters, the issue of spin crossing points for the (smif)Fe=CMe_2/CH_4 reaction coordinate was not pursued.

In closing this section, we must note that while the ^{6}(smif)-Fe=O complex showed the most favorable energetics for C−H activation, such a four-coordinate system would be synthetically challenging to access. Given the low coordination at the metal (ferryl intermediates in cytochrome P450 are envisaged as six-coordinate complexes[76−78]), the oxo ligand is unprotected by

dx.doi.org/10.1021/ic400804x | Inorg. Chem. 2013, 52, 8106−8113

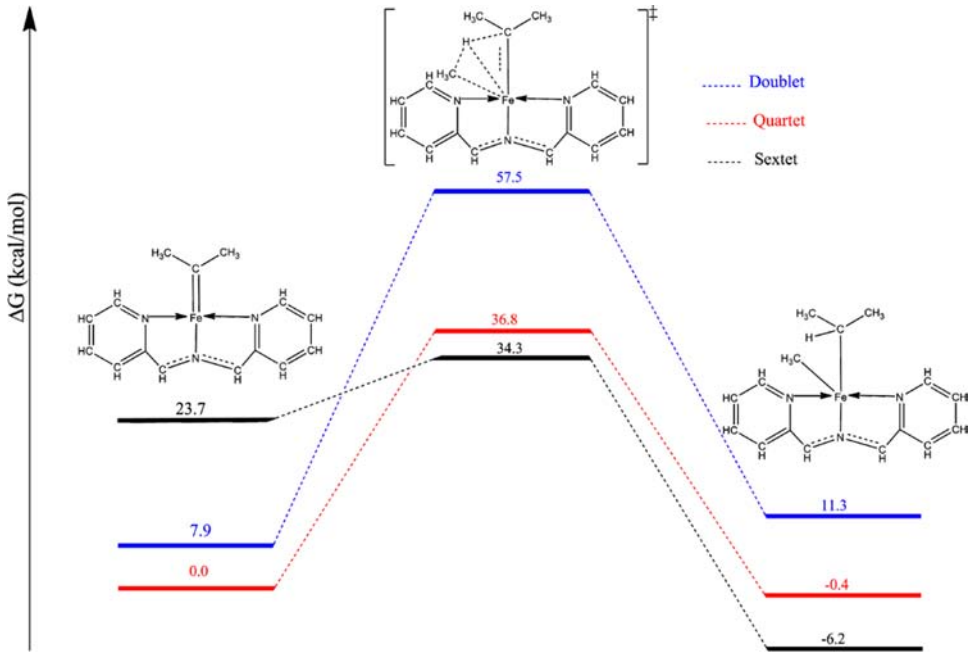

Figure 5. Reaction coordinate for (smif)Fe=CMe_2 + CH_4. ^{s}(smif)Fe=CMe_2 + CH_4 → ^{s}[(smif)Fe(CH_3)(H)(CMe_2)]‡ → ^{s}(smif)Fe(CH_3)-($CHMe_2$). Initial energy values are with respect to the calculated ground state ^{4}(smif)Fe=CMe_2.

Table 4. Calculated Lowest-Energy Spin States, Thermodynamics, and Kinetics of (smif)M=NMe + CH_4 → (smif)M(CH_3)(NHMe) Reaction for 3d (Fe) and 4/5d (Ru, Os, and Pd) Metals

	reactant spin state	TS spin state	product spin state	$\Delta G^‡$ (kcal/mol)	ΔG_{rxn} (kcal/mol)	TS type
Fe	sextet	sextet	sextet	29.1	−9.6	$[2_\sigma+2_\pi]$
Ru	doublet	doublet	doublet	45.7	−5.7	[HAA]
Os	doublet	doublet	doublet	55.2	2.3	[HAA]
Pd	doublet	doublet	doublet	31.7	22.5	[HAA]

any substituents, unlike the nitrogen of the Fe-imide complex. Hence, one could easily conceive of side reactions, e.g., with the solvent or other metal complexes, or the formation of μ-oxo or bimetallic species during the course of any experiments. Thus, from a computational and experimental perspective, the Fe-imide complex remains the most promising target complex modeled thus far.

C. Comparison of Iron to Precious Metal Congeners and Palladium. The (smif)Fe=NMe complex was compared to precious metal congeners using the calculated reaction parameters of the first-row transition metals thus far modeled. Because of the lack of availability of suitable all-electron basis sets for the precious metals and the greater importance of relativistic effects for the latter, a pseudopotential valence basis set,[63−65] comparable to the 6-31+G(d) all-electron basis set used to model 3d complexes, was used for ruthenium, osmium, and palladium. As before, the 6-31+G(d) basis set was used for the main group elements.

As with the Fe and Ni complexes, spin conservation was observed with all the precious metals. This was as expected given the propensity of heavier metals to be in low-spin states because of their higher ligand field splittings. The computed activation barriers and reaction energies are significantly higher than those calculated for the ^{6}(smif)Fe=NMe complex (Tables 4 and 5). For ruthenium and osmium, TS searches using both $[2_\sigma+2_\pi]$ and [HAA] initial guess geometries resulted in stationary points. However, the HAA TSs were ∼3 kcal/mol lower than the $[2_\sigma+2_\pi]$ TS for both metals. In the absence of metric constraints, a $[2_\sigma+2_\pi]$ TS search for the Pd system converges to the HAA TS.

Table 5. Calculated Thermodynamics of the (smif)M=NMe + CH_4 → (smif)M-NHMe + $CH_3^•$ Reaction

	reactant spin state	HAA[a] spin state	ΔG_{HAA} (kcal/mol)
Fe	sextet	quintet	15.6
Ru	doublet	triplet	29.2
Os	doublet	triplet	45.3
Pd	doublet	singlet	17.9

[a]HAA = hydrogen atom abstraction.

The large differences in HAA free energies (Table 5) for the iron complex versus the heavy metal congeners loosely correlate with the higher free-energy barriers (Table 4) for methane C−H activation. This result suggests that the lower barrier for the iron complex is due to weaker metal−nitrogen π-bond energies for the 3d metal imides as compared to those of their 4d and 5d analogues (Table 5). Note that the computed HAA free energies of the Fe- and Pd-imides are similar (Table 5), as are their methane activation barriers (Table 4), lending credence to the proposal that metal−nitrogen π-bond energies are a key discriminating parameter in determining the barriers to methane C−H activation via either a $[2_\sigma+2_\pi]$ or an HAA pathway.

dx.doi.org/10.1021/ic400804x | Inorg. Chem. 2013, 52, 8106−8113

4. SUMMARY, CONCLUSIONS, AND PROSPECTUS

The goal of this research is to model complexes using a combination of potentially noninnocent ligands and base metals that may serve to identify novel complexes that may activate C−H bonds under mild conditions. The dipyridylazaallyl (smif) ligand, a reported noninnocent ligand with high ligand field strength,[39,52−55] was used in an attempt to confer the electronic properties of precious (4d and 5d) metals onto the base (3d) metals studied. Four first-row transition metals were studied (Fe, Co, Ni, and Cu) with the activating ligand methylimide (NMe). Two routes were considered for each (smif)M═NMe + CH_4 reaction: one via a $[2_\sigma+2_\pi]$-type transition state, the other via a hydrogen atom abstraction transition state. Several important conclusions were reached with respect to metal-mediated C−H activation, which are summarized here.

(1) Of the four 3d metals modeled, the (smif)Fe═NMe complex showed the most favorable kinetics and thermodynamics for methane C−H activation. It was the only 3d metal studied that displayed a preference for a $[2_\sigma+2_\pi]$ TS. The preferred transition state for methane C−H activation gradually shifted from the $[2_\sigma+2_\pi]$ to the [HAA] archetype from left to right among the metals studied. Although the activation barriers for the Co, Ni, and Cu complexes were higher than that of the Fe complex, the actual values decreased among the three metals for which an HAA TS was the preferred mode of C−H activation: Co > Ni > Cu. This is similar to the trend observed by Pierpont and Cundari[16] in their study of HAA by (β-diketiminate)M═NR complexes.

It is interesting to note that all four HAA reactions ((smif)M═NMe + CH_4 → (smif)M—NHMe + $CH_3^\bullet$) to produce a three-coordinate amide intermediate are nearly identical in their endergonicity [$\Delta G_{HAA} \sim 17 \pm 1$ kcal/mol (Table 2)] Free energies for the (smif)M═NMe + CH_4 → (smif)M(CH_3)(NHMe) reactions to produce a four-coordinate amide product, on the other hand, span a calculated range of 27 kcal/mol for the 3d metals studied (Table 1). Hence, one may infer that the M—CH_3 bond strengths, estimated from the differences in these computed free energies ($BDFE_{MCH_3} \sim \Delta G_{HAA} - \Delta G_{rxn}$), are a significant discriminant in the reactivity of these late 3d metal smif complexes. Using the data in Tables 1 and 2 gives M—CH_3 bond dissociation free energies estimated from the reaction (smif)M(CH_3)—NHMe → (smif)M—NHMe + $CH_3^\bullet$ of 25 (Fe), 16 (Co), 1 (Ni), and 5 (Cu) kcal/mol. While the difficulties in accurate measurement of transition metal-ligand bond energies via experimental and computational means are well-known,[34−38,79−81] the present computations suggest that the weaker M—CH_3 bonds of Ni and Cu result in the HAA pathway being preferred.

Presumably, factors such as sterics and entropy would favor an HAA over a $[2_\sigma+2_\pi]$ pathway in the absence of other mitigating factors. Rationalization of the change in TS preference as a function of metal was also sought in terms of spin density on the metal-nitrogen active site of (smif)M═NMe (Table 6). No obvious correlations were discerned. However, and perhaps more interestingly, computed spin densities suggest that it was not the smif but rather the NMe that was acting as the noninnocent ligand! There was significant spin density on the nitrogen of the activating ligand in the ground state of all imide complexes studied here. For the copper complex, $N_{spin} \sim 1.3$ e^-, while the spin density on the imide N was ∼0.9−1.0 e^- for the other metals. This disposition of the unpaired spin density was suggestive of an imidyl ($NR^{\bullet-}$) description of the ground state (smif)M═NMe complexes for these late 3d metals with the copper being more heavily weighted than the others toward a nitrene ($NR^{\bullet\bullet}$) description because of its $N_{spin} > 1$.

Table 6. Calculated Spin Densities on the Metal and Nitrogen of the NMe Ligand in the (smif)M═NMe Reactant

	total spin density	metal spin density	nitrogen spin density
^{6}(smif)Fe═NMe	5.0	3.8	1.0
^{3}(smif)Co═NMe	2.0	1.0	0.9
^{2}(smif)Ni═NMe	1.0	0.0	1.0
^{3}(smif)Cu═NMe	2.0	0.5	1.3

(2) The active ligand, NMe, was replaced by two isoelectronic ligands, oxo and dimethylcarbene. The (smif)Fe═O complex showed improved energetics versus (smif)Fe═NMe; however, side reactions are expected to be more problematic for a catalytic cycle in which (smif)Fe═O is an active species. The (smif)Fe═CMe_2 model, although yielding a methane C−H activation energy higher than those of the oxo and imide complexes, was interesting. Of the iron complexes studied, the dimethylcarbene complex preferred a spin state (quartet) lower than the sextet spin state observed for other Fe complexes. The dimethylcarbene complex also exhibited a spin flip going from reactant to transition state, whereas spin conservation is observed for the other modeled Fe complexes.

Perhaps the most obvious trend that can be discerned is that a more electronegative activating ligand yields a lower methane C−H activation barrier. It is tempting to ascribe this to greater polarization of the $M^{\delta+}$═$E^{\delta-}$ active site inducing greater $C^{\delta-}$—$H^{\delta+}$ polarization, perhaps hinting at some deprotonation character of the C−H activation TS. However, an analysis of calculated atomic charges in the transition states shows little difference among the 3d metals. A more sensitive analysis via a Hammett-type study would be intriguing in regard to this supposition, and such studies are underway in our laboratory.

(3) Comparison of the (smif)Fe═NMe complex to ruthenium-, osmium-, and palladium-imide complexes showed improved C−H activation ability (lower $\Delta G^\ddagger$, more exergonic ΔG_{rxn}) of the Fe complex over the precious metals. The (smif)Fe═NMe complex preferred the $[2_\sigma+2_\pi]$ route, while the ruthenium and osmium complexes preferred the HAA route. Carsch and Cundari[1] also observed similar trends in transition state preference for group 6 oxo complexes, i.e., heavier metals prefer an HAA over a $[2_\sigma+2_\pi]$ TS pathway. One plausible rationalization that may be proffered for the shift in TS mechanism within a triad is that the four-coordinate amide product of [2+2] C−H addition is formally M^{3+}. However, HAA entails a reduction of the metal center to the stable M^{2+} formal oxidation state for the (smif)M—NHMe product.

We hypothesize that the higher C−H activation barriers for the 3d metals stem more from the lower metal−nitrogen π-bond energies that must be invested in the 3d metals than from the energies invested in 4d and 5d metals, leading to lower activation barriers for the former. The HAA free energies (conversion of a three-coordinate imide to a three-coordinate amide) correlate reasonably well with the higher free-energy barriers for methane C−H activation (Figure 6). This result suggests that the lower barrier for (smif)Fe═NMe is due to metal−nitrogen π-bond energies for the 3d metal imides that

dx.doi.org/10.1021/ic400804x | Inorg. Chem. 2013, 52, 8106−8113

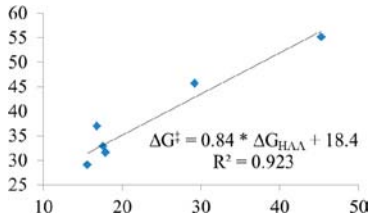

Figure 6. Plot of ΔG_{HAA} (x axis in kilocalories per mole, computed free energy of the reaction (smif)M═NMe + CH_4 → (smif)M—NHMe + $CH_3^{\bullet}$) versus $\Delta G^{\ddagger}$ (y axis in kilocalories per mole, computed free-energy barrier for methane C−H activation by (smif)M═NMe, M = Fe, Co, Ni, Cu, Ru, Os, and Pd). Note that the Cu and Pd data points are nearly coincident.

are weaker than those of their 4d and 5d analogues. Note that the computed HAA free energies of the Fe/Cu and Pd imides are similar (Table 5), as are their methane activation barriers (Table 4), lending credence to the proposal that metal−nitrogen π-bond energies are a key discriminating parameter in determining the barriers to methane C−H activation via either a $[2_\sigma+2_\pi]$ or an HAA pathway.

Overall, the (smif)Fe═NMe complex shows favorable kinetics and thermodynamics for C−H activation, and the present computations suggest LFe═NR with smif and related pincer-like ligands to be attractive synthetic targets. Wolczanski et al. have reported the synthesis of a four-coordinate amide, (smif)FeN(TMS)$_2$,[52] but, to our knowledge, no related complexes with a multiply bonded ligand. However, Fe-imides have been isolated and strongly implicated as reactive intermediates in C−H bond activation and functionalization by, among others, Holland,[69,82,83] Betley,[32,66,71] Chirik,[25−28] and their co-workers. Hence, the models proposed herein seem synthetically viable. What is less clear, but perhaps more intriguing, is if the superiority of Fe versus the other 3d congeners analogues modeled here is a reflection of the intrinsic superiority of a $[2_\sigma+2_\pi]$ mechanism vis-à-vis an HAA route to methane activation/functionalization. Modeling to address this question more definitively is underway in our laboratory.

■ ASSOCIATED CONTENT

Ⓢ Supporting Information

Details on activating and supporting ligand modifications, including figures, data, and precious metal transition state geometries. This material is available free of charge via the Internet at http://pubs.acs.org.

■ AUTHOR INFORMATION

Corresponding Author

*E-mail: t@unt.edu.

Notes

The authors declare no competing financial interest.

■ ACKNOWLEDGMENTS

The authors acknowledge financial support from the National Science Foundation (CHE-1057758).

■ REFERENCES

(1) Carsch, K. M.; Cundari, T. R. *Comput. Theor. Chem.* **2012**, *980*, 133.
(2) Cundari, T. R. *Organometallics* **1994**, *13*, 2987.
(3) Foley, N. A.; Gunnoe, T. B.; Cundari, T. R.; Boyle, P. D.; Petersen, J. L. *Angew. Chem., Int. Ed.* **2008**, *47*, 726.
(4) Labinger, J. A.; Bercaw, J. E. *Nature* **2002**, *417*, 507.
(5) Arndtsen, B. A.; Bergman, R. G.; Mobley, T. A.; Peterson, T. H. *Acc. Chem. Res.* **1995**, *28*, 154.
(6) Schaller, C. P.; Wolczanski, P. T. *Inorg. Chem.* **1993**, *32*, 131.
(7) Walsh, P. J.; Hollander, F. J.; Bergman, R. G. *J. Am. Chem. Soc.* **1988**, *110*, 8729.
(8) Cundari, T. R.; Grimes, T. V.; Gunnoe, T. B. *J. Am. Chem. Soc.* **2007**, *129*, 13172.
(9) Kalyani, D.; Deprez, N. R.; Desai, L. V.; Sanford, M. S. *J. Am. Chem. Soc.* **2005**, *127*, 7330.
(10) Figg, T. M.; Cundari, T. R.; Gunnoe, T. B. *Organometallics* **2011**, *30*, 3779.
(11) Ritleng, V.; Sirlin, C.; Pfeffer, M. *Chem. Rev.* **2002**, *102*, 1731.
(12) Wiese, S.; Badiei, Y. M.; Gephart, R. T.; Mossin, S.; Varonka, M. S.; Melzer, M. M.; Meyer, K.; Cundari, T. R.; Warren, T. H. *Angew. Chem., Int. Ed.* **2010**, *49*, 8850.
(13) Schwarz, H. *Angew. Chem., Int. Ed.* **2011**, *50*, 10096.
(14) Cummins, C. C.; Baxter, S. M.; Wolczanski, P. T. *J. Am. Chem. Soc.* **1988**, *110*, 8731.
(15) Ke, Z. F.; Cundari, T. R. *Organometallics* **2010**, *29*, 821.
(16) Pierpont, A. W.; Cundari, T. R. *Inorg. Chem.* **2010**, *49*, 2038.
(17) Prince, B. M.; Cundari, T. R. *Organometallics* **2012**, *31*, 1042.
(18) Hazari, N.; Mountford, P. *Acc. Chem. Res.* **2005**, *38*, 839.
(19) Mindiola, D. J. *Acc. Chem. Res.* **2006**, *39*, 813.
(20) Cummins, C. C.; Schaller, C. P.; Van Duyne, G. D.; Wolczanski, P. T.; Chan, A. W. E.; Hoffmann, R. *J. Am. Chem. Soc.* **1991**, *113*, 2985.
(21) Scott, J.; Basuli, T.; Fout, A. R.; Huffman, J. C.; Mindiola, D. J. *Angew. Chem., Int. Ed.* **2008**, *47*, 8502.
(22) Toomey, H. E.; Pun, D.; Veiros, L. F.; Chirik, P. J. *Organometallics* **2008**, *27*, 872.
(23) Laskowski, C. A.; Miller, A. J. M.; Hillhouse, G. L.; Cundari, T. R. *J. Am. Chem. Soc.* **2011**, *133*, 771.
(24) Polse, J. L.; Andersen, R. A.; Bergman, R. G. *J. Am. Chem. Soc.* **1998**, *120*, 13405.
(25) Bart, S. C.; Bowman, A. C.; Lobkovsky, E.; Chirik, P. J. *J. Am. Chem. Soc.* **2007**, *129*, 7212.
(26) Bowman, A. C.; Bart, S. C.; Heinemann, F. W.; Meyer, K.; Chirik, P. J. *Inorg. Chem.* **2009**, *48*, 5587.
(27) Bowman, A. C.; Milsmann, C.; Bill, E.; Turner, Z. R.; Lobkovsky, E.; DeBeer, S.; Wieghardt, K.; Chirik, P. J. *J. Am. Chem. Soc.* **2011**, *133*, 17353.
(28) Bart, S. C.; Lobkovsky, E.; Bill, E.; Chirik, P. J. *J. Am. Chem. Soc.* **2006**, *128*, 5302.
(29) Shay, D. T.; Yap, G. P. A.; Zakharov, L. N.; Rheingold, A. L.; Theopold, K. H. *Angew. Chem., Int. Ed.* **2005**, *44*, 1508.
(30) Dobbs, D. A.; Bergman, R. G. *J. Am. Chem. Soc.* **1993**, *115*, 3836.
(31) Mindiola, D. J.; Hillhouse, G. L. *J. Am. Chem. Soc.* **2001**, *123*, 4623.
(32) Brown, S. D.; Betley, T. A.; Peters, J. C. *J. Am. Chem. Soc.* **2003**, *125*, 322.
(33) Kogut, E.; Wiencko, H. L.; Zhang, L. B.; Cordeau, D. E.; Warren, T. H. *J. Am. Chem. Soc.* **2005**, *127*, 11248.
(34) Aquilante, F.; Malmqvist, P. A.; Pedersen, T. B.; Ghosh, A.; Roos, B. O. *J. Chem. Theory Comput.* **2008**, *4*, 694.
(35) Ghosh, A.; Gonzalez, E.; Tangen, E.; Roos, B. O. *J. Phys. Chem. A* **2008**, *112*, 12792.
(36) Tangen, E.; Conradie, J.; Ghosh, A. *J. Chem. Theory Comput.* **2007**, *3*, 448.
(37) Wasbotten, I. H.; Ghosh, A. *Inorg. Chem.* **2007**, *46*, 7890.
(38) Conradie, J.; Ghosh, A. *J. Chem. Theory Comput.* **2007**, *3*, 689.
(39) Frazier, B. A.; Wolczanski, P. T.; Lobkovsky, E. B. *Inorg. Chem.* **2009**, *48*, 11576.
(40) Hirsekorn, K. F.; Hulley, E. B.; Wolczanski, P. T.; Cundari, T. R. *J. Am. Chem. Soc.* **2008**, *130*, 1183.
(41) Chirik, P. J.; Wieghardt, K. *Science* **2010**, *327*, 794.
(42) Nguyen, A. I.; Zarkesh, R. A.; Lacy, D. C.; Thorson, M. K.; Heyduk, A. F. *Chem. Sci.* **2011**, *2*, 166.

(43) Heyduk, A. F.; Zarkesh, R. A.; Nguyen, A. I. *Inorg. Chem.* **2011**, *50*, 9849.
(44) Ray, K.; Petrenko, T.; Wieghardt, K.; Neese, F. *Dalton Trans.* **2007**, 1552.
(45) Cowley, R. E.; Bill, E.; Neese, F.; Brennessel, W. W.; Holland, P. L. *Inorg. Chem.* **2009**, *48*, 4828.
(46) Lippert, C. A.; Hardcastle, K. I.; Soper, J. D. *Inorg. Chem.* **2011**, *50*, 9864.
(47) Nawn, G.; Waldie, K. M.; Oakley, S. R.; Peters, B. D.; Mandel, D.; Patrick, B. O.; McDonald, R.; Hicks, R. G. *Inorg. Chem.* **2011**, *50*, 9826.
(48) Boyer, J. L.; Rochford, J.; Tsai, M. K.; Muckerman, J. T.; Fujita, E. *Coord. Chem. Rev.* **2010**, *254*, 309.
(49) Butin, K. P.; Beloglazkina, Y. K.; Zyk, N. V. *Usp. Khim.* **2005**, *74*, 585.
(50) Lever, A. B. P.; Gorelsky, S. I. *Struct. Bonding (Berlin)* **2004**, *107*, 77.
(51) Boyer, J. L.; Cundari, T. R.; DeYonker, N. J.; Rauchfuss, T. B.; Wilson, S. R. *Inorg. Chem.* **2009**, *48*, 638.
(52) Frazier, B. A.; Wolczanski, P. T.; Lobkovsky, E. B.; Cundari, T. R. *J. Am. Chem. Soc.* **2009**, *131*, 3428.
(53) Frazier, B. A.; Bartholomew, E. R.; Wolczanski, P. T.; DeBeer, S.; Santiago-Berrios, M.; Abruna, H. D.; Lobkovsky, E. B.; Bart, S. C.; Mossin, S.; Meyer, K.; Cundari, T. R. *Inorg. Chem.* **2011**, *50*, 12414.
(54) Hachmann, J.; Frazier, B. A.; Wolczanski, P. T.; Chan, G. K. L. *ChemPhysChem* **2011**, *12*, 3236.
(55) Volpe, E. C.; Wolczanski, P. T.; Lobkovsky, E. B. *Organometallics* **2010**, *29*, 364.
(56) Cowley, R. E.; Christian, G. J.; Brennessel, W. W.; Neese, F.; Holland, P. L. *Eur. J. Inorg. Chem.* **2012**, *2012*, 479.
(57) Frisch, M. J.; et al. *Gaussian 09*; Gaussian, Inc.: Wallingford, CT, 2009.
(58) Zhao, Y.; Truhlar, D. G. *Theor. Chem. Acc.* **2008**, *120*, 215.
(59) Petersson, G. A.; Bennett, A.; Tensfeldt, T. G.; Al-Laham, M. A.; Shirley, W. A.; Mantzaris, J. *J. Chem. Phys.* **1988**, *89*, 2193.
(60) Petersson, G. A.; Al-Laham, M. A. *J. Chem. Phys.* **1991**, *94*, 6081.
(61) Dugan, T. R.; Sun, X.; Rybak-Akimova, E. V.; Olatunji-Ojo, O.; Cundari, T. R.; Holland, P. L. *J. Am. Chem. Soc.* **2011**, *133*, 12418.
(62) Frazier, B. A.; Wolczanski, P. T.; Keresztes, I.; DeBeer, S.; Lobkovsky, E. B.; Pierpont, A. W.; Cundari, T. R. *Inorg. Chem.* **2012**, *51*, 8177.
(63) Stevens, W. J.; Basch, H.; Krauss, M. *J. Chem. Phys.* **1984**, *81*, 6026.
(64) Stevens, W. J.; Krauss, M.; Basch, H.; Jasien, P. G. *Can. J. Chem.* **1992**, *70*, 612.
(65) Cundari, T. R.; Stevens, W. J. *J. Chem. Phys.* **1993**, *98*, 5555.
(66) Cundari, T. R.; Jimenez-Halla, J. O. C.; Morello, G. R.; Vaddadi, S. *J. Am. Chem. Soc.* **2008**, *130*, 13051.
(67) Cundari, T. R.; Pierpont, A. W.; Vaddadi, S. *J. Organomet. Chem.* **2007**, *692*, 4551.
(68) Adams, C. S.; Legzdins, P.; Tran, E. *J. Am. Chem. Soc.* **2001**, *123*, 612.
(69) Eckert, N. A.; Vaddadi, S.; Stoian, S.; Lachicotte, R. J.; Cundari, T. R.; Holland, P. L. *Angew. Chem., Int. Ed.* **2006**, *45*, 6868.
(70) Vaddadi, S. Computational Studies of Coordinatively Unsaturated Transition Metal Complexes. Ph.D. Dissertation, University of North Texas, Denton, TX, 2006.
(71) King, E. R.; Hennessy, E. T.; Betley, T. A. *J. Am. Chem. Soc.* **2011**, *133*, 4917.
(72) Klinker, E. J.; Shaik, S.; Hirao, H.; Que, L. *Angew. Chem., Int. Ed.* **2009**, *48*, 1291.
(73) De Angelis, F.; Jin, N.; Car, R.; Groves, J. T. *Inorg. Chem.* **2006**, *45*, 4268.
(74) Cowley, R. E.; Eckert, N. A.; Vaddadi, S.; Figg, T. M.; Cundari, T. R.; Holland, P. L. *J. Am. Chem. Soc.* **2011**, *133*, 9796.
(75) Schöneboom, J. C.; Neese, F.; Thiel, W. *J. Am. Chem. Soc.* **2005**, *127*, 5840.
(76) Poulos, T. L.; Finzel, B. C.; Howard, A. J. *Biochemistry* **1986**, *25*, 5314.
(77) Hasemann, C. A.; Ravichandran, K. G.; Peterson, J. A.; Deisenhofer, J. *J. Mol. Biol.* **1994**, *236*, 1169.
(78) Cryle, M. J.; Meinhart, A.; Schlichting, I. *J. Biol. Chem.* **2010**, *285*, 24562.
(79) Fey, N.; Ridgway, B. M.; Jover, J.; McMullin, C. L.; Harvey, J. N. *Dalton Trans.* **2011**, *40*, 11184.
(80) Craciun, R.; Vincent, A. J.; Shaughnessy, K. H.; Dixon, D. A. *Inorg. Chem.* **2010**, *49*, 5546.
(81) Hallowita, N.; Udonkang, E.; Ruan, C. H.; Frieler, C. E.; Rodgers, M. T. *Int. J. Mass Spectrom.* **2009**, *283*, 35.
(82) Cowley, R. E.; DeYonker, N. J.; Eckert, N. A.; Cundari, T. R.; DeBeer, S.; Bill, E.; Ottenwaelder, X.; Flaschenriem, C.; Holland, P. L. *Inorg. Chem.* **2010**, *49*, 6172.
(83) Cowley, R. E.; Holland, P. L. *Inorg. Chem.* **2012**, *51*, 8352.